*Proc. Natl. Acad. Sci. USA*
Vol. 80, pp. 6114–6118, October 1983
Neurobiology

# Autoradiographic localization of a binding protein(s) specific for prostaglandin $D_2$ in rat brain

**(receptor/*in vitro* labeling/computer-assisted image processing/color coding/regional distribution)**

AKIRA YAMASHITA*, YASUYOSHI WATANABE†, AND OSAMU HAYAISHI*‡

*Department of Medical Chemistry, Kyoto University Faculty of Medicine, and †Radioisotope Research Center, Kyoto University, Kyoto 606, Japan

*Contributed by Osamu Hayaishi, July 5, 1983*

**ABSTRACT** **The specific [$^3$H]prostaglandin (PG) $D_2$ binding was detected by using the slide-mounted sections of rat brain fixed by perfusion with 2% paraformaldehyde. The binding was reversible, saturable, high affinity, $Na^+$ dependent, and highly specific for $PGD_2$. These binding characteristics are essentially similar to those observed with the synaptic membrane of rat brain as previously reported. Using autoradiographic image analyses by computerized densitometry and color coding, we visualized the localization of [$^3$H]$PGD_2$ binding in rat brain. A high density of the binding sites was observed in the cerebral cortex, preoptic area, amygdala, hypothalamic nuclei (arcuate nucleus, ventromedial nucleus, and posterior hypothalamic nucleus), thalamic nuclei (reuniens nucleus and rhomboid nucleus), hippocampus, pineal body, and cerebellar cortex. The binding was not significantly observed in the striatum and also was negative in the white matter, arachnoid membranes, and vasculatures.**

Prostaglandin (PG) $D_2$ is the major PG in the brain of rat and other mammalian species (1–3). The enzymes catalyzing the biosynthesis (4) and metabolic inactivation of $PGD_2$ (5) have been found in the brain and spinal cord and have been investigated in detail (3, 6). The administration of $PGD_2$ into rat brain caused hypothermia (7), induced sleep (8, 9), and inhibited the pulsatile secretion of luteinizing hormone (10). These effects are probably mediated by the interaction between $PGD_2$ and its binding protein (11) that may be linked to the adenylate cyclase system (12). In the present study, we visualized the distribution pattern of [$^3$H]$PGD_2$ binding in rat brain by *in vitro* labeling, computerized densitometry, and color coding as described by Quirion *et al.* (13). The distribution of the binding protein is unique in comparison with the receptor distribution of other neuroactive substances reported so far (13–20).

## MATERIALS AND METHODS

**Tissue Preparation.** Male Wister rats (≈300 g) were injected intraperitoneally with indomethacin (1 mg/kg of body weight) to minimize a postmortem endogenous synthesis of PGs. After 1 hr, the rats were perfused with 200 ml of cold 10 mM sodium phosphate-buffered saline (pH 7.4) ($P_i$/NaCl) containing 20 $\mu$g of indomethacin per ml. Then, the brains were fixed *in situ* by perfusion with 200 ml of cold $P_i$/NaCl containing 2% paraformaldehyde, followed by perfusion with 200 ml of indomethacin-containing $P_i$/NaCl. The brains were rapidly removed, and 1- to 3-mm slices of appropriate regions were immersed in OCT (Tissue-Tek II, Miles), frozen at −40°C, and cut into serial 10-$\mu$m-thick coronal sections at −14°C in a cryostat. The sections were thaw-mounted onto acid-washed and gelatin-coated glass slides. Materials prepared in this way can be stored for at least 1 week at 4°C without a significant change of specific [$^3$H]$PGD_2$ binding activity.

**[$^3$H]$PGD_2$ Binding.** All procedures of [$^3$H]$PGD_2$ binding assay were performed at 4°C. The tissue sections were preincubated in 50 mM Tris·HCl buffer (pH 7.4) containing 0.1 M NaCl (buffer A) for 1 hr. After excess solution around the tissue was removed with filter paper, the solution (100 $\mu$l) of 20 nM [$^3$H]$PGD_2$ in buffer A was poured over the tissue sections. After the incubation in a moist chamber with a gentle shaking for 20 min, the slides were rinsed in four changes of buffer A, each for 15 sec, quickly splashed with distilled water, wiped with filter paper to remove excess water around the tissue, and air-dried. Total and nonspecific bindings were determined in the consecutive sections by incubation with [$^3$H]$PGD_2$ in the absence and presence of 100 $\mu$M unlabeled $PGD_2$, respectively.

**Biochemical Experiments.** The sections were scraped from the slides with a razor blade and placed in scintillation vials. After the tissue was dissolved in 1 ml of Protosol (New England Nuclear), the radioactivity was measured in 10 ml of Triton X-100/toluene scintilator (11). The radioactivity of the specific binding was calculated by subtracting that of the nonspecific binding from that of the total binding. The nonspecific binding amounted to about 70% of the total binding. The slices of diencephalon (thalamus and hypothalamus) were used because Shimizu *et al.* had reported the presence of a large amount of specific $PGD_2$ binding in this region with the $P_2$ fraction of rat brain (11). Four diencephalons were embedded in a plastic vessel with OCT, in such a way that two were cut coronally from anterior to posterior hypothalamus, and the other two were cut in the opposite direction. All values are expressed as the means of four to five determinations.

The specific binding increased linearly with the thickness (4–20 $\mu$m) of sections, when the sections were incubated under the standard assay conditions as described above. No loss of the specific binding was observed with fixation by perfusion with paraformaldehyde solutions up to 4%.

**Analysis of Tissue-Bound [$^3$H]$PGD_2$.** The stability of bound [$^3$H]$PGD_2$ during the binding assay was checked as follows. The sections (100 slides) were incubated with 20 nM [$^3$H]$PGD_2$ as described above, and the tissues were air-dried, scraped off, and transferred into a homogenizer. Tissue-bound [$^3$H]$PGD_2$ was extracted twice with 5 ml of buffer A containing 100 $\mu$M $PGD_2$ and twice with 5 ml of 50% ethanol. The combined extracts were purified by the method of Narumiya *et al.* (2) with Sep-Pak $C_{18}$ cartridges (Waters Associates). Overall recovery of the radioactive substance throughout the extraction steps was 55%. The final extract was dried up, dissolved in 200 $\mu$l of diethyl ether, and applied to a thin-layer chromatographic silica

The publication costs of this article were defrayed in part by page charge payment. This article must therefore be hereby marked "*advertisement*" in accordance with 18 U.S.C. §1734 solely to indicate this fact.

Abbreviation: PG, prostaglandin.

‡ To whom reprint requests should be addressed at: Osaka Medical College, 2-7 Daigaku-cho, Takatsuki, Osaka-fu 569, Japan.

gel plate with solvent systems I (ethyl acetate/isooctane/acetic acid/water, 11:5:2:10, vol/vol; the upper layer) and II (benzene/dioxan/acetic acid, 20:10:1, vol/vol).

**Autoradiography.** After being dried in a dessicator, the slides were juxtaposed tightly with tritium-sensitive films (Ultrafilm, LKB) and stored at 4°C for 4–8 weeks. After the exposure, the film was processed in Kodak D19 at 20°C for 5 min and then fixed for 5 min. Autoradiographs of the total and nonspecific bindings were concomitantly analyzed by a computer-assisted image-processing system. The specific binding sites can be visualized as the subtracted images between those of total and nonspecific bindings. The binding sites were identified by Nissl staining on the same section after the autoradiography with reference to the stereotaxic atlas of rat brain as described by Paxinos and Watson (21).

**Computer-Assisted Image-Processing System.** The computerized system was adopted to process the autoradiographic data by the method of Goochee *et al.* (22). This includes a rotating-drum scanning densitometer, a color image display, and a microcomputer system. The rotating-drum scanning densitometer (model 2605, Kimoto, Tokyo) was used to convert the photometric data from the autoradiographs into digital forms. The digitalized data were designated to be parallel with the optical density between 0 and 3. Sampling pitches were 50 $\mu$m, and aperture sizes for data collecting were 75 × 75 $\mu$m. The array of optical density readings was processed through a microcomputer (NOVA IV/X, Data General, Westboro, MA). For the decrease of the scanning noise, the sum of density levels of six images at each point was obtained. These data were converted to pseudocolor images and transferred to a color image display (512 × 512 elements, model M-201, Kimoto).

**Materials.** [5,6,8,9,12,14,15-$^3$H(N)]$PGD_2$ (100 Ci/mmol; 1 Ci = 3.7 × $10^{10}$ Bq) was purchased from New England Nuclear. The radiochemical purity was >97% as judged by thin-layer chromatography with solvent systems as described above. Unlabeled PGs and thromboxane $B_2$ were generous gifts from Ono Pharmaceutical (Osaka, Japan).

## RESULTS

**Biochemical Studies.** Fig. 1*A* shows the time course of the specific [$^3$H]$PGD_2$ binding with 10-$\mu$m-thick sections. The [$^3$H]$PGD_2$ binding increased with time and was saturated at 20 min. As shown in Fig. 1*B*, the time course of the dissociation of [$^3$H]$PGD_2$ from the sections is represented by a straight line when plotted semilogarithmically. The half-time for the dissociation ($t_{1/2}$) was 16 min. The specific binding was saturable with the concentration of [$^3$H]$PGD_2$ (80 nM) (Fig. 2). The half-maximal saturating concentration was 33 nM, and the number of binding sites at the saturation was 9.8 fmol/mg of tissue. These values are comparable to those observed with synaptic membranes of rat brain ($K_d$ = 28 × $10^{-9}$ M) or the $P_2$ fraction of hypothalamus ($B_{max}$ = 124 fmol/mg of protein) (11).

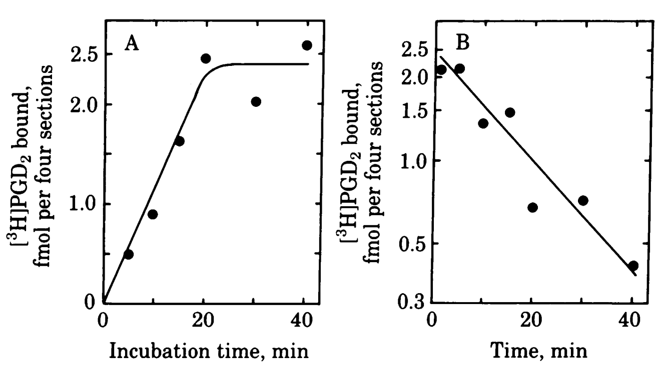


FIG. 1. Time courses of [$^3$H]$PGD_2$ association to (*A*) and dissociation from (*B*) the sections of rat diencephalon. (*A*) The sections (10-$\mu$m thick) were incubated with 20 nM [$^3$H]$PGD_2$ at 4°C for indicated times, followed by four 15-sec washings in buffer A. (*B*) After a 20-min incubation at 4°C, the slides were rinsed in four changes of buffer A within indicated times at 4°C. The radioactivities of the sections were measured as described in the text. Specific binding was calculated by subtracting the nonspecific binding (in the presence of 100 $\mu$M $PGD_2$) from the total binding (in the absence of excess $PGD_2$).

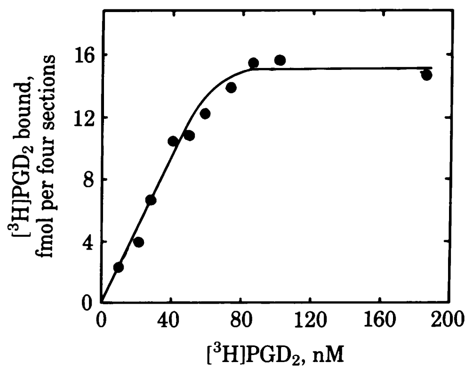


FIG. 2. Saturation curve of specific [$^3$H]$PGD_2$ binding to the sections of rat diencephalon. The sections were incubated in varied concentrations of [$^3$H]$PGD_2$ at 4°C for 20 min, followed by four 15-sec washings at 4°C. The experiments were replicated twice with similar results.

To evaluate the specificity of the $PGD_2$ binding, we tested the effect of the addition of various PGs (1 $\mu$M of $PGD_2$, $PGD_2$ methyl ester, $PGD_1$, $PGF_{2\alpha}$, $PGB_2$, $PGE_1$, $PGE_2$, $PGI_2$, 6-keto-$PGF_{1\alpha}$, or thromboxane $B_2$) to the incubation mixture on the [$^3$H]$PGD_2$ binding (20 nM). $PGD_2$ and its methyl ester were most potent (70.5 ± 9.7% and 54.5 ± 7.7% inhibition, respectively) among various PGs examined. A slight inhibition was observed by the addition of $PGD_1$ (32.7 ± 3.8%) and $PGF_{2\alpha}$ (26.7 ± 5.4%). Other PGs examined did not cause a significant inhibition.

Because $PGD_2$ binding to synaptic membranes was found to be markedly reduced in the absence of a sufficient concentration of sodium ion (11), we also altered the concentration of $Na^+$ in the incubation mixture with the slide-mounted tissue sections. Maximum $PGD_2$ binding was observed in the presence of 25–100 mM NaCl, and the specific binding was reduced in the absence of NaCl or in the presence of >200 mM NaCl (Fig. 3). After slide-mounted tissue sections were boiled in buffer A for 10 min, the total and nonspecific bindings in-

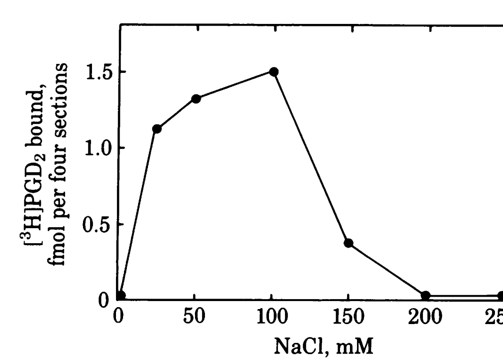


FIG. 3. Effects of the concentration of sodium ion in the incubation mixture on the specific [$^3$H]$PGD_2$ binding to the sections of rat diencephalon. Incubations were carried out under the standard assay conditions as described in the text, except that 0.1 M NaCl was replaced by varying concentrations of NaCl. The experiments were repeated twice with similar results.

creased 2- to 3-fold, and a significant amount of specific binding was no longer detected.

When the radioactive substance(s) bound to the tissues was analyzed after the incubation, the radioactive peaks other than $[^3H]PGD_2$ were not significantly detected (the radioactive purity of the peak ≈ 90%).

**Autoradiographical Studies.** Serial coronal sections of rat brain, including nine typical brain areas indicated in Fig. 4, were incubated with 20 nM $[^3H]PGD_2$ in the absence or presence of 100 $\mu$M unlabeled $PGD_2$. Autoradiographs were analyzed by a computer-assisted image-processing system (Fig. 5). The average of the density of the nonspecific binding in the coronal section was around 70% of that of the total binding. This ratio obtained by the densitometry is well compatible with that obtained by the calculation of the radioactivities of the slide-mounted tissues as already mentioned.

In all sections examined, specific binding sites for $PGD_2$ were restricted to the gray matter. High densities were present in the cerebral cortex (Fig. 5 *B–G*) and hypothalamus (Fig. 5 *C–E*). The specific binding was not significantly observed in the striatum (Fig. 5 *B* and *C*), the white matter, arachnoid membrane, and vasculature.

In Fig. 5*A* [bregma 6.7 mm in the atlas (21)], the specific binding was observed in the mitral cell layer or in the internal plexiform layer of the olfactory bulb, or in both. In Fig. 5*B* (bregma 0.2 to about −0.3 mm), the preoptic area, lateral septal nucleus, piriform cortex (primary olfactory cortex), and cingulate cortex exhibited the high $PGD_2$ binding, and the corpus callosum, fornix, anterior commisure, and optic tract did not exhibit significant binding. In Fig. 5*C* (bregma −1.3 mm), the binding was observed in the anterior hypothalamic area, anterior thalamic nuclei (reuniens nucleus and anteromedial nucleus), substantia innominata, and frontopariental cortex and was not observed in the corpus callosum, fornix, internal capsule, and globus pallidus. In Fig. 5*D* (bregma −2.3 to about −2.8 mm), high density of the binding was observed in the frontoparietal cortex (motor area), posterior cingulate cortex, hippocampus (ammon's horn and dentate gyrus), amygdaloid nuclei, hypothalamic nuclei (arcuate nucleus and ventromedial nucleus), and thalamic nuclei (reuniens nucleus and rhomboid nucleus). The internal capsule was negative. In Fig. 5*E* (bregma −4.3 to about −4.8 mm), high density of the binding was observed in the frontoparietal cortex, hippocampus, substantia nigra, posterior hypothalamic nucleus, and mammillary nuclei. In Fig. 5*F* (bregma −5.3 to about −5.8 mm), high density was observed in the retrosplenial cortex, temporal cortex (auditory area), superior colliculus (superficial gray layer), and hippocampus. Moderate density was observed in the substantia nigra and periventricular gray. In Fig. 5*G* (bregma −7.8 mm), high density of the binding was observed in the pineal body and striate cortex, and moderate density was in the superior colliculus and periventricular gray. The pons was negative, except that low density of the binding was observed in the median raphe nucleus and pontine reticular nucleus. In Fig. 5*H* (bregma −11.3 mm), moderate density of the binding was observed in the cerebellar cortex, and low density was observed in the lateral cervical nucleus (dentate nucleus) and pontine nuclei (dorsal cochlear nucleus, prepositus hypoglossal nucleus, medial vestibular nucleus, facial nucleus, and raphe magnus nucleus). On the other hand, the cerebellar medulla and fiber tracts (spinal tract of trigeminal nerve, ascending fibers of facial nerve, and medial longitudinal fasciculus) were negative. In Fig. 5*I* (bregma −12.3 mm), significant binding was observed in the cerebellar cortex, and low density was in the prepositus hypoglossal nuclei and medial vestibular nuclei.

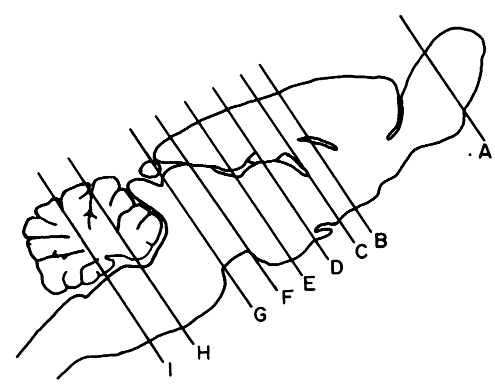


FIG. 4. Schematic drawing of the sagittal plane of the rat brain. The rat brain was cut at each coronal plane indicated by 9 straight lines in the figure. These coronal sections were used for the present autoradiographic study.

## DISCUSSION

An autoradiographical method using an *in vitro* labeling technique has been utilized to visualize the localization of the receptors of various neurotransmitters and drugs (13–20). The method has the advantage of not only the precise control for the labeling conditions but also the assessment of the binding characteristics. In the present study, we have demonstrated that $[^3H]PGD_2$ binding with the slide-mounted tissue sections has several characteristics similar to those with synaptic membrane (11); the binding was reversible, saturable, high affinity, $Na^+$ dependent, inactivated by heat, and highly specific for $PGD_2$. The binding was clearly distinguishable from that to PGD synthetase or $PGD_2$ dehydrogenase judging from the difference between the $K_d$ value of the binding protein ($33 \times 10^{-9}$ M) and the $K_m$ values for $PGD_2$ with PGD synthetase ($8 \times 10^{-6}$ M) (4) and $PGD_2$ dehydrogenase ($70 \times 10^{-6}$ M) (6). Although $PGD_2$ was reported to bind to some blood cells (11, 23), the blood cells were excluded from the preparation by perfusion in the present study. The ratio (30%) of the specific binding to total binding with slide-mounted sections was lower than that (60–70%) with the synaptic membranes but was in the same order as that observed with $P_2$ fraction (30%) (11). These results imply that the specific binding shown in the present study well reflects the binding of $PGD_2$ to the specific binding protein in the synaptic membranes of rat brain.

A comparably high content of nonspecific $PGD_2$ binding forced us to analyze the autoradiographs by a computer-assisted image-processing system of Quirion *et al.* (13). Although the density of the nonspecific binding also was not distributed uniformly throughout the brain (Fig. 5 *A–I Lower*), we infer that a tentative distribution of the specific $PGD_2$ binding was obtained. In several discrete areas, we performed the subtraction

FIG. 5 (*on next page*). Visualization of $[^3H]PGD_2$ binding sites in the rat brain. Nine paired autoradiographs were prepared and converted to color images by computerized densitometry and color coding as described in the text. The upper picture of each figure represents the image of total binding upon incubation with 20 nM $[^3H]PGD_2$ and the lower one represents that of nonspecific binding upon incubation with 20 nM $[^3H]$-$PGD_2$/100 $\mu$M unlabeled $PGD_2$. The optical densities of the autoradiographs are indicated beside the color coding bar. MCL, mitral cell layer; IPL, internal plexiform layer; RE, reuniens nucleus; AHA, anterior hypothalamic area; ARH, arcuate nucleus; VMH, ventomedial nucleus; S. NIGRA, substantia nigra; CS, superior colliculus; PVG, periventricular gray; NPH, prepositus hypoglossal nucleus; NVM, medial vestibular nucleus; VII, facial nucleus.

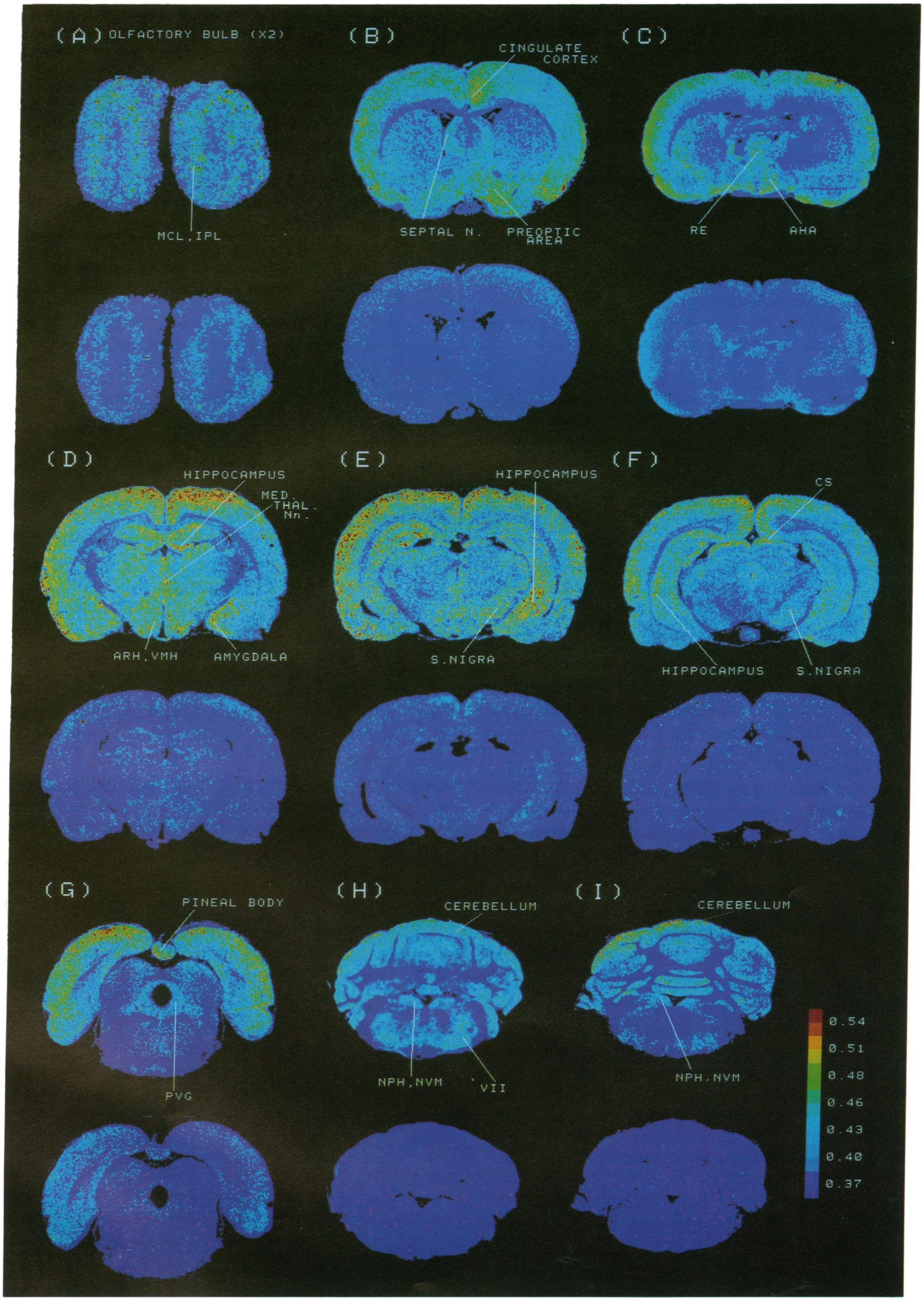


FIG. 5. (*Legend appears at the bottom of the preceding page.*)

from the average density of the total binding to that of the nonspecific binding. The subtracted values in the area coded in yellow to red color in the images of the total binding were higher than those in the area coded in blue to green in the images of the total binding. Thus, the relative densities might not be significantly altered even if the direct subtraction between the densities of two images at all corresponding data points could be obtained in the future study.

The present study shows the unique localization of $PGD_2$ binding sites, in comparison with the localizations of known neurotransmitter receptors (13–20). High density of $PGD_2$ binding was observed in the cerebral and cerebellar cortices, the members of the limbic system (preoptic area, septum, olfactory bulb, hippocampus, and amygdala), and several nuclei of diencephalon. Scarce binding was observed in the striatum and the nuclei of the brain stem. The regional differences of dense $PGD_2$ binding between the hemispheres are apparent in the reconstituted images from the autoradiographs (especially in Fig. 5 *B*, *C*, and *E*). At present, it is unsolved whether these side-to-side differences reflect uneven distribution of the binding protein *in vivo* or are due to some technical error, such as the slightly inclined sectioning to the coronal plane. The latter possibility was suggested in other works (13, 24).

Our observed localization of $PGD_2$ binding protein provides some rational explanation for several central (pharmacological and physiological) effects of $PGD_2$ so far known. For example, the microinjection of $PGD_2$ to preoptic area or the anterior hypothalamic area produces the hypothermal (7) and sleep-promoting effects (8). These areas are reported to be the thermal center (25) and one of the centers of sleep (26). In agreement with this, we observed high densities of the $PGD_2$ binding in these areas. Another example is the inhibition of pulsatile secretion of luteinizing hormone by intraventricular injection of $PGD_2$ (10). This response is thought to be caused by the reduction of the release of luteinizing hormone releasing hormone from the hypothalamic nuclei. We found high densities of $PGD_2$ binding in the arcuate nucleus and some other areas related to the secretion of luteinizing hormone releasing hormone. Another example of the correlation between the location of the binding protein and central effects of $PGD_2$ was our observation of high densities of $PGD_2$ binding in various members of the limbic system. $PGD_2$ has significant effects on autonomic responses (27) and locomotor activities (28). Other unknown neurophysiological effects of $PGD_2$ may be predicted through the present study in relation to the limbic function (29) such as emotional and sexual behaviors and learning.

Mitral cell is the principal cell in the olfactory bulb, which is the secondary neuron in the olfactory pathway. We found high density of the $PGD_2$ binding around the mitral cell layer. This result suggests a regulatory role of $PGD_2$ in the input of olfaction. More interestingly, inhibitory recurrent synapses between granular cells and mitral cells are rich in this layer. Recently, we have found a high density of the $PGD_2$ binding in the Purkinje cell layer of the pig cerebellum (30). The Purkinje cell layer also contains numerous synapses from the inhibitory neurons. $PGD_2$ may act as one of the neurotransmitters or neuromodulators in the inhibitory recurrent neuronal circuits.

We thank Mr. C. Miyakozawa, Mr. A. Terakubo, and Miss T. Nakayama of Kimoto Co., Ltd., for their help with computer analyses and Dr. T. Shimizu and Dr. S. Narumiya in our department for useful discussions. This work was supported in part by a Grant-in-Aid for Scientific Research from the Ministry of Education, Science and Culture of Japan and by grants from the Japanese Foundation of Metabolism and Diseases, Fujiwara Memorial Foundation, the Japan Heart Foundation, and Shimadzu Science Foundation.

1. Wolfe, L. S. (1982) *J. Neurochem.* **38,** 1–14.
2. Narumiya, S., Ogorochi, T., Nakao, K. & Hayaishi, O. (1982) *Life Sci.* **31,** 2093–2103.
3. Hayaishi, O. (1983) in *Advances in Prostaglandin, Thromboxane, and Leukotriene Research*, eds. Samuelsson, B., Paoletti, R. & Ramwell, P. (Raven, New York), Vol. 12, pp. 333–337.
4. Shimizu, T., Yamamoto, S. & Hayaishi, O. (1979) *J. Biol. Chem.* **254,** 5222–5228.
5. Watanabe, K., Shimizu, T., Iguchi, S., Wakatsuka, H., Hayashi, M. & Hayaishi, O. (1980) *J. Biol. Chem.* **255,** 1779–1782.
6. Tokumoto, H., Watanabe, K., Fukushima, D., Shimizu, T. & Hayaishi, O. (1982) *J. Biol. Chem.* **257,** 13576–13580.
7. Ueno, R., Narumiya, S., Ogorochi, T., Nakayama, T., Ishikawa, Y. & Hayaishi, O. (1982) *Proc. Natl. Acad. Sci. USA* **79,** 6093–6097.
8. Ueno, R., Ishikawa, Y., Nakayama, T. & Hayaishi, O. (1982) *Biochem. Biophys. Res. Commun.* **109,** 576–582.
9. Ueno, R., Honda, K., Inoué, S. & Hayaishi, O. (1983) *Proc. Natl. Acad. Sci. USA* **80,** 1735–1737.
10. Kinoshita, F., Nakai, Y., Katakami, H., Imura, H., Shimizu, T. & Hayaishi, O. (1982) *Endocrinology* **110,** 2207–2209.
11. Shimizu, T., Yamashita, A. & Hayaishi, O. (1982) *J. Biol. Chem.* **257,** 13570–13575.
12. Shimizu, T., Mizuno, N., Amano, T. & Hayaishi, O. (1979) *Proc. Natl. Acad. Sci. USA* **76,** 6231–6234.
13. Quirion, R., Hammer, R. P., Jr., Herkenham, M. & Pert, C. B. (1981) *Proc. Natl. Acad. Sci. USA* **78,** 5881–5885.
14. Kuhar, M. J. & Yamamura, H. I. (1976) *Brain Res.* **110,** 229–243.
15. Atweh, S. F. & Kuhar, M. J. (1977) *Brain Res.* **134,** 393–405.
16. Young, W. S., III, & Kuhar, M. J. (1980) *J. Pharmacol. Exp. Ther.* **212,** 337–346.
17. Young, W. S., III, & Kuhar, M. J. (1980) *Proc. Natl. Acad. Sci. USA* **77,** 1696–1700.
18. Palacios, J. M., Niehoff, D. L. & Kuhar, M. J. (1981) *Brain Res.* **213,** 277–289.
19. Palacios, J. M., Wamsley, J. K. & Kuhar, M. J. (1981) *Neuroscience* **6,** 15–37.
20. Palacios, J. M., Wamsley, J. K. & Kuhar, M. J. (1981) *Brain Res.* **222,** 285–307.
21. Paxinos, G. & Watson, C. (1982) *The Rat Brain in Stereotaxic Coordinates* (Academic, New York).
22. Goochee, C., Rasband, W. & Sokoloff, L. (1980) *Ann. Neurol.* **7,** 359–370.
23. Cooper, B. & Ahern, D. (1979) *J. Clin. Invest.* **64,** 586–590.
24. Monaghan, D. T. & Cotman, C. W. (1982) *Brain Res.* **252,** 91–100.
25. Bligh, J. (1979) *Neuroscience* **4,** 1213–1236.
26. Krueger, J. M., Pappenheimer, J. R. & Karnovsky, M. L. (1982) *Proc. Natl. Acad. Sci. USA* **79,** 6102–6106.
27. Hemker, D. P. & Aiken, J. W. (1980) *Prostaglandins* **20,** 321–332.
28. Laychock, S. G., Johnson, D. N. & Harris, L. S. (1980) *Pharmacol. Biochem. Behav.* **12,** 747–754.
29. Kupfermann, I. (1981) in *Principles of Neural Science*, eds. Kandel, E. R. & Schwartz, J. H. (Elsevier/North-Holland, New York), pp. 433–449.
30. Watanabe, Y., Yamashita, A., Tokumoto, H. & Hayaishi, O. (1983) *Proc. Natl. Acad. Sci. USA* **80,** 4542–4545.